

## **ROLL SPEED AND WEB TENSION REGULATION USING TWO DEGREE OF FREEDOM CONTROL SYSTEMS**

**By**

**Pramod R. Raul and Prabhakar R. Pagilla  
Oklahoma State University  
USA**

### **ABSTRACT**

In this paper, we first consider the problem of load speed regulation in a two inertia system consisting of a motor shaft connected to the load shaft via a mechanical transmission. The problem is reminiscent of a material roll (load) connected to the motor shaft through a belt-pulley and gear transmission system. In typical industrial speed control systems, the motor shaft speed is controlled under the assumption that the load shaft speed is indirectly controlled at its desired value scaled by the transmission ratio. In the presence of the transmission dynamics introduced by compliance and backlash, regulation of motor shaft speed does not translate to regulation of roll speed. The problem is further exacerbated when there are disturbances on the roll. One must consider the transmission dynamics in developing a control system that can provide the desired performance for the roll speed. We propose a two degree of freedom control system that utilizes measurement of motor shaft and roll shaft angular velocities in developing a control action necessary to regulate the roll speed. The control system consists of both feedback and model-based feedforward actions. The model-based feedforward action is generated by utilizing the model and adaptively estimating the disturbances on the roll. Experimental results conducted on a web machine indicate improved roll speed regulation in the presence of disturbances, which will be presented and discussed. Utilizing the improved roll speed regulation scheme a tension control strategy is also proposed and experiments were conducted with web transport. Experimental results indicate improved tension regulation with such a strategy.

## NOMENCLATURE

$A_w$	:	Area of cross-section of web
$b_L$	:	Viscous friction coefficient of load
$b_m$	:	Viscous friction coefficient of motor
$E$	:	Modulus of elasticity of web material
$G_R$	:	Gear ratio
$J_L$	:	Moment of inertia of load
$J_m$	:	Moment of inertia of motor
$K_b$	:	Stiffness of the belt
$K_{pm}$	:	Proportional gain of motor speed control
$K_{im}$	:	Integral gain of motor speed control
$K_{pL}$	:	Proportional gain of load speed control
$K_{iL}$	:	Integral gain of load speed control
$L_i$	:	Length of $i^{th}$ web span
$R_{Pi}$	:	Radii of pulleys
$R_{gi}$	:	Radii of gears
$t_i$	:	Web tension of $i^{th}$ span
$v_i$	:	Velocity of $i^{th}$ roller
$\omega_L$	:	Angular velocity of load
$\omega_m$	:	Angular velocity of motor
$\theta_L$	:	Angular displacements of the motor
$\theta_m$	:	Angular displacements of the load
$\tau_L$	:	Load torque disturbance
$\tau_m$	:	Motor torque

## INTRODUCTION

Mechanical transmissions are widely employed in various industries where the mechanical power is typically transmitted from motor shafts to load shafts. Control of load speed is essential in many applications. When rigid transmissions are employed, there is no dynamics between the motor shaft and the load shaft, and typically the motor shaft speed is controlled to control the speed of the load shaft. However, due to the transmission dynamics, resulting from the compliance of belt as well as long shafts in the transmission, regulating load shaft speed is not the same as regulating motor shaft speed. The use of gear box and belt in transmission of R2R system introduce undesired oscillations in web tension. In the presence of such a transmission, practicing engineers are often confronted with the question of whether to use (i) motor speed feedback to control load speed as is done in conventional practice, or (ii) use load speed feedback, or (iii) use a combination of motor and load speed feedback.

There is a large body of literature on the characteristics of belt drives and design of mechanisms using belt drives. The disturbances generated by belt compliance, gear backlash, shaft torsional compliance or external disturbances on load side must be compensated to achieve desired load speed regulation

performance. A linear model with backlash and belt compliance was presented in [6] and is considered in this work for further analysis. A common controller that is employed for regulation of load speed for a two-inertia elastic system is PI control which provides limited performance in the presence of disturbances. In order to overcome these limitations, a load torque observer is suggested in [5]. Though this technique is useful in preventing limit cycles, load speed remained uncontrolled in the presence of uncertainties. In [6], it is shown that employing only load speed feedback in the speed control system results in an unstable system which is also discussed in this work and further analyzed. The simultaneous feedback from motor and load speed feedback is first proposed in [7], which also suggested application of a preload to close the backlash gap; a simulation study showed that limit cycles are attenuated if the applied preload is smaller than backlash gap. In [8], a two degree freedom fuzzy controller, consisting of a feedback fuzzy controller and a feedforward acceleration compensator, is proposed to control a belt drive precision positioning table.

A load and motor speed model which consider belt-pulley and gear pair power transmission is considered in this paper. In the given model, motor torque is considered as input while speed of the driven roller (load speed) as the output of the system. A simultaneous load and motor speed feedback control scheme is considered for obtaining better load speed regulation by attenuating disturbances. Further, in order to reject periodic disturbances, an add-on adaptive feedforward (AFF) control action along with motor and load speed feedback (two degree freedom control) is considered.

The proposed two degree freedom load speed regulation scheme is extended to web tension control. Comparative experimental results with an existing industrial control scheme and proposed control scheme are presented in frequency and time domains, and further discussions are provided. The proposed load speed regulation scheme is further implemented in the rewind section in order to investigate web tension control in the presence of disturbances.

The remainder of the paper describes the model of the system, the motor speed feedback only and load speed feedback only control schemes, a control scheme that utilizes both motor and load speed feedback, an add-on adaptive feedforward compensation to reject load speed disturbances, the extension of proposed load speed regulation scheme to web tension control.

## MODEL OF THE SYSTEM

A schematic of a belt-pulley and gear transmission system connecting the motor with the load is shown in Figure 1. To derive the governing equations for this system we consider the action of the belt in transmitting power. For a given direction of rotation of the pulley, the belt has a tight side and a slack side as shown in Figure 1. It is assumed that the transmission of power is taking place on the tight side and the transport of the belt is taking place on the slack side. Under this assumption, the net change in tension on the slack side will be much smaller than that in the tight side and thus may be ignored. The tight side of

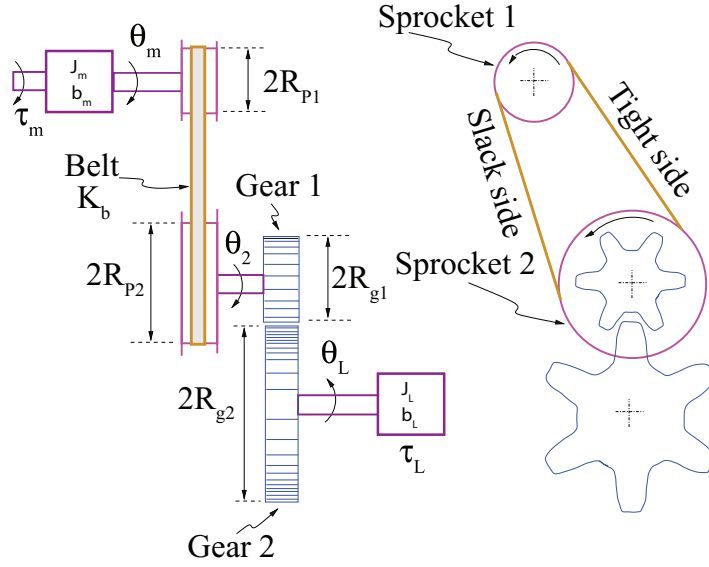


Figure 1 – Schematic of a belt-pulley and gear-pair transmission system

the belt can then be modeled as a spring with spring constant of  $K_b$ . For given angular displacements  $\theta_m$  and  $\theta_L$ , the net elongation of the tight side of the belt can be written as  $(R_{P1}\theta_m - G_R R_{P2}\theta_L)$ , where  $G_R = R_{g2}/R_{g1}$  is gear ratio. Because of this elongation, the driving pulley experiences a torque of  $(R_{P1}\theta_m - G_R R_{P2}\theta_L)K_b R_{P1}$  and the driven pulley experiences a torque of  $(R_{P1}\theta_m - G_R R_{P2}\theta_L)G_R R_{P2}K_b$ . Under the assumption that the inertias of the pulleys and gears are much smaller than the motor and the load, the governing equations of motion for the motor-side inertia and the load-side inertia are given by [6]

$$J_m \ddot{\theta}_m + b_m \dot{\theta}_m + R_{P1}K_b(R_{P1}\theta_m - G_R R_{P2}\theta_L) = \tau_m, \quad \{1a\}$$

$$J_L \ddot{\theta}_L + b_L \dot{\theta}_L - G_R R_{P2}K_b(R_{P1}\theta_m - G_R R_{P2}\theta_L) = \tau_L. \quad \{1b\}$$

A block diagram representation of the system given by {1} is provided in Figure 2; note that this block diagram represents the open-loop system and the two “loops” appearing in the block diagram represent the interconnections in {1}. The open-loop transfer functions from the motor torque signal  $\tau_m$  to the motor speed  $\omega_m$  and load speed  $\omega_L$  are given by

$$G_{\tau_m \omega_m}(s) \triangleq \frac{\omega_m(s)}{\tau_m(s)} = \frac{J_L s^2 + b_L s + G_R^2 R_{P2}^2 K_b}{D(s)}, \quad \{2a\}$$

$$G_{\tau_m \omega_L}(s) \triangleq \frac{\omega_L(s)}{\tau_m(s)} = \frac{G_R R_{P1} R_{P2} K_b}{D(s)}, \quad \{2b\}$$

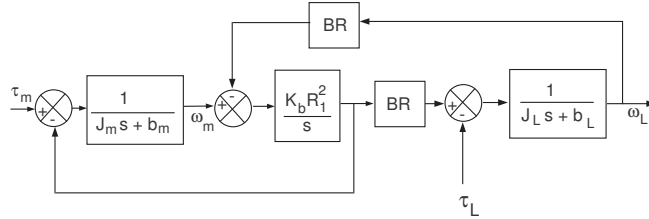


Figure 2 – Block diagram of the belt-pulley and gear transmission system;  $BR$  denotes the overall speed ratio,  $BR = (R_{P2}/R_{P1})G_R$ .

where

$$D(s) = J_m J_L s^3 + (b_L J_m + J_L b_m) s^2 + (K_b J_{eq} + b_m b_L) s + K_b b_{eq}, \quad \{3a\}$$

$$J_{eq} = G_R^2 R_{P2}^2 J_m + R_{P1}^2 J_L, \quad \{3b\}$$

$$b_{eq} = G_R^2 R_{P2}^2 b_m + R_{P1}^2 b_L. \quad \{3c\}$$

The goal is to control the load speed  $\omega_L$ . In the following we will discuss the closed-loop control systems that consider three scenarios: (i) pure motor speed feedback, (ii) pure load speed feedback, and (iii) a combination of motor and load speed feedback.

### MOTOR SPEED FEEDBACK CONTROL SCHEME

It is common to control load speed by using the measurement of motor speed  $\omega_m$  as feedback. This control scheme is shown in Figure 3. The control structure is designed to regulate motor speed  $\omega_m$  to the reference  $\omega_{rm}$ , and thereby indirectly regulate load speed  $\omega_L$ .

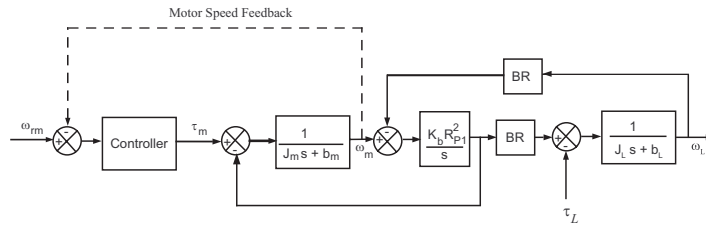


Figure 3 – Motor speed feedback control scheme

We consider the often used Proportional-Integral (PI) control action which is given by

$$\tau_m = K_{pm}(\omega_{rm} - \omega_m) + K_{im} \int (\omega_{rm} - \omega_m) d\tau. \quad \{4\}$$

With this control law, the closed-loop transfer function from  $\omega_{rm}$  to  $\omega_L$  is obtained as

$$\frac{\omega_L(s)}{\omega_{rm}(s)} = \frac{(G_R R_{P1} R_{P2} K_b / J_m J_L)(s K_{pm} + K_{im})}{\Psi_m(s)}, \quad \{5\}$$

where

$$\begin{aligned} \Psi_m(s) &= s^4 + c_3 s^3 + c_2 s^2 + c_1 s + c_0, \\ c_3 &= \frac{(b_m J_L + J_m b_L + K_{pm} J_L)}{J_m J_L}, \\ c_2 &= \frac{(K_b J_{eq} + b_m b_L + K_{pm} b_L + K_{im} J_L)}{J_m J_L}, \\ c_1 &= \frac{(K_b b_{eq} + G_R^2 R_{P2}^2 K_b K_{pm} + K_{im} b_L)}{J_m J_L}, \\ c_0 &= \frac{G_R^2 R_{P2}^2 K_b K_{im}}{J_m J_L}. \end{aligned} \quad \{6\}$$

Note the the coefficients  $c_0$  to  $c_3$  depend on the controller gains. It is possible to place poles by selecting controller parameter values.

Parameter sensitivity analysis: We consider the singular perturbation method for analyzing such a system with the small parameter equal to the reciprocal of the square root of the belt stiffness  $K_b$ . For conducting singular perturbation analysis, we express the equations in the form

$$\dot{x} = A_{11}x + A_{12}z, \quad x(t_0) = x^0 \quad \{7a\}$$

$$\varepsilon \dot{z} = A_{21}x + A_{22}z, \quad z(t_0) = z^0 \quad \{7b\}$$

where  $x$  and  $z$  are the states of the slow and the fast subsystems, respectively, and  $\varepsilon$  is the small parameter; for our system we will consider  $\varepsilon^2 = 1/K_b$ . The elements of the matrices  $A_{ij}$  may depend on  $\varepsilon$ . However, to use the singular perturbation method, the matrix  $A_{22}$  needs to be nonsingular [2] at  $\varepsilon = 0$ . A natural choice of the state variables for the singular perturbation analysis is  $\theta_m$ ,  $\dot{\theta}_m$ ,  $\theta_L$  and  $\dot{\theta}_L$ . However, with this choice of the state variables, the matrix  $A_{22}$  becomes singular at  $\varepsilon = 0$ . To obtain a state-space representation in the form that would enable the use of the singular perturbation method, we consider the following transformation of variables [6] :

$$\theta_c \triangleq \frac{J_m \theta_m + J_L G_R (R_{P2}/R_{P1}) \theta_L}{J_m + J_L}, \quad \{8a\}$$

$$\theta_s \triangleq \theta_m - G_R (R_{P2}/R_{P1}) \theta_L. \quad \{8b\}$$

The variable  $\theta_c$  is a weighted average of angular displacements ( $\theta_m$  and  $\theta_L$ ) referred to the motor side and the variable  $\theta_s$  is difference between the angular displacements ( $\theta_m$  and  $\theta_L$ ) referred to the motor side; transformations similar to these have been used in prior studies of two inertia systems, see for example [3]. The idea of the weighted average of the displacements arises naturally in the case

of a translational system wherein  $\theta_c$  represents the position of the centroid of the masses. Now, choosing the state variables as  $x = [\theta_c, \dot{\theta}_c]^\top$  and  $z = [\theta_s/\varepsilon^2, \dot{\theta}_s/\varepsilon]^\top$ , the state space representation of the system is obtained in the form given by {7}. The characteristic equation for the transformed system can be factored as [2]

$$\Psi_m(s, \varepsilon) \approx \frac{1}{\varepsilon^2} \Psi_{ms}(s, \varepsilon) \Psi_{mf}(p, \varepsilon) = 0 \quad \{9\}$$

with

$$\Psi_{ms}(s, \varepsilon) \triangleq \det[sI_2 - (A_{11} - A_{12}L(\varepsilon))], \quad \{10a\}$$

$$\Psi_{mf}(p, \varepsilon) \triangleq \det[pI_2 - (A_{22} + \varepsilon L(\varepsilon)A_{12})] \quad \{10b\}$$

where  $\Psi_{ms}(s, \varepsilon)$  is the characteristic polynomial for the slow subsystem and  $\Psi_{mf}(p, \varepsilon)$  is the characteristic polynomial of the fast subsystem exhibited in the high-frequency scale  $p = \varepsilon s$ . The matrix  $L(\varepsilon)$  is obtained using the iterative scheme given in [2].

Using the matrices  $A_{ij}$ , the slow and the fast characteristic polynomials are obtained as

$$\Psi_{ms}(s, \varepsilon) \approx s^2 + \alpha_1 s + \alpha_0, \quad \{11a\}$$

$$\Psi_{mf}(p, \varepsilon) \approx p^2 + \alpha'_1 p + \alpha'_2 \quad \{11b\}$$

where

$$\begin{aligned} \alpha_1 &= \frac{G_R^2 R_{P2}^2 b_m + R_{P1}^2 b_L + G_R^2 R_{P2}^2 K_{pm}}{G_R^2 R_{P2}^2 J_m + R_{P1}^2 J_L}, \\ \alpha_0 &= \frac{G_R^2 R_{P2}^2 K_{im}}{G_R^2 R_{P2}^2 J_m + R_{P1}^2 J_L}, \\ \alpha'_1 &= \frac{G_R^2 R_{P2}^2 K_{pm} J_L}{J_m (G_R^2 R_{P2}^2 J_m + R_{P1}^2 J_L)} \varepsilon, \\ \alpha'_2 &= \frac{G_R^2 R_{P2}^2 J_L + R_{P1}^2 J_m}{J_m J_L}. \end{aligned} \quad \{12\}$$

Equation {11} indicates that both the fast and the slow subsystems are stable for all  $K_{pm}, K_{im} > 0$ . This indicates that irrespective of the value of the belt stiffness, this speed control system is stable.

## LOAD SPEED FEEDBACK CONTROL SCHEME

One can employ the load speed feedback scheme shown in Figure 4, where the measured variable is  $\omega_L$ . This seems to have the advantage of directly controlling load speed and attenuating the effect of the disturbance  $\tau_L$ . The feedback law is given by

$$\tau_m = K_{pL}(\omega_{rL} - \omega_L) + K_{iL} \int (\omega_{rL} - \omega_L) d\tau, \quad \{13\}$$

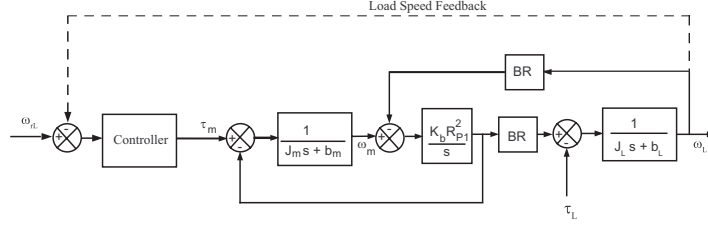


Figure 4 – Load speed feedback control scheme

and the closed-loop transfer function from  $\omega_{rL}$  to  $\omega_L$  is obtained as

$$\frac{\omega_L(s)}{\omega_{rL}(s)} = \frac{(G_R R_{P1} R_{P2} K_b / J_m J_L)(s K_{pL} + K_{iL})}{\Psi_L(s)} \quad \{14\}$$

where

$$\begin{aligned} \Psi_L(s) &= s^4 + d_3 s^3 + d_2 s^2 + d_1 s + d_0, \\ d_3 &= \frac{(b_m J_L + J_m b_L)}{J_m J_L}, \\ d_2 &= \frac{(K_b J_{eq} + b_m b_L)}{J_m J_L}, \\ d_1 &= \frac{(K_b b_{eq} + G_R R_{P1} R_{P2} K_b K_{pL})}{J_m J_L}, \\ d_0 &= \frac{G_R R_{P1} R_{P2} K_b K_{iL}}{J_m J_L}. \end{aligned} \quad \{15\}$$

Singular perturbation analysis pertaining to this control scheme results in the following slow and fast characteristic polynomials:

$$\Psi_{Is}(s, \epsilon) \approx s^2 + \beta_1 s + \beta_0 \quad \{16a\}$$

$$\Psi_{If}(p, \epsilon) \approx p^2 - \beta'_1 p + \beta'_0 \quad \{16b\}$$

where

$$\begin{aligned} \beta_1 &= \frac{G_R^2 R_{P2}^2 b_m + R_{P1}^2 b_L + G_R R_{P2} R_{P1} K_{pL}}{G_R^2 R_{P2}^2 J_m + R_{P1}^2 J_L}, \\ \beta_0 &= \frac{G_R R_{P2} R_{P1} K_{iL}}{G_R^2 R_{P2}^2 J_m + R_{P1}^2 J_L}, \\ \beta'_1 &= \frac{G_R^2 R_{P2}^2 b_m + R_{P1}^2 b_L + G_R^2 R_{P2}^2 K_{pL}}{G_R^2 R_{P2}^2 J_m + R_{P1}^2 J_L} \epsilon, \\ \beta'_0 &= \frac{G_R^2 R_{P2}^2 J_L + R_{P1}^2 J_m}{J_m J_L}. \end{aligned} \quad \{17\}$$

Note that the slow subsystem is stable for all  $K_{pL}, K_{iL} > 0$ . However, the fast subsystem is unstable for all  $K_{pL} > 0$  and  $K_{iL} > 0$ . Also, note that the



characteristic polynomials given by equations {11b} and {16b} are identical when  $\varepsilon = 0$ . Thus, analyzing the limiting case of an infinitely stiff belt, that is,  $\varepsilon = 0$  will not reveal the instability exhibited by {16b}.

The load speed  $\omega_L$  can attain steady-state only when motor speed  $\omega_m$  attains steady-state first. This is shown by the following differential equation,

$$J_L \ddot{\omega}_L + b_L \dot{\omega}_L + R_{P2}^2 K_b \omega_L = R_{P1} R_{P2} K_b \omega_m, \quad \{18\}$$

which is obtained by differentiating {1b}. Even when the motor speed  $\omega_m$  attains steady-state,  $\omega_L$  continues to exhibit damped oscillations. Thus, by measuring only  $\omega_L$  and using the control law given by {13}, the damped oscillations of the load speed cannot be distinguished from oscillations due to the motor speed fluctuations. Therefore, the controller reacts also to the damped oscillations of the load speed, hence avoiding  $\omega_m$  (and as a consequences also  $\omega_l$ ) to settle to its steady-state value. Thus, the control law given by {13} does not present a desirable situation.

### SIMULTANEOUS MOTOR AND LOAD SPEED FEEDBACK CONTROL SCHEME

In this scheme, the load speed control corrects directly the torque input to the system as shown in Figure 5. The closed-loop transfer function from  $\omega_{rL}$  to

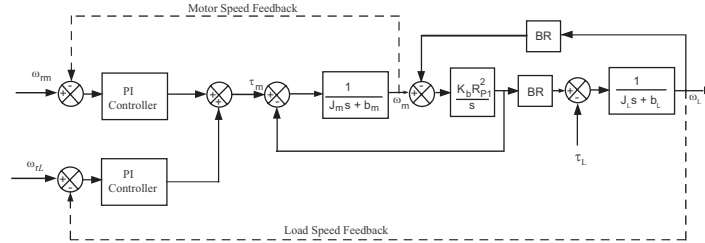


Figure 5 – Simultaneous motor and load speed feedback scheme: Torque mode

$\omega_L$  is given by

$$\frac{\omega_L(s)}{\omega_{rL}(s)} = \frac{\alpha_{mL}(s)}{\Psi_{mL}(s)} \quad \{19\}$$

where

$$\begin{aligned} \alpha_{mL}(s) &= a_1 s + a_0, \\ a_1 &= \frac{(G_R R_{P1} R_{P2} K_b K_{pl} + G_R R_{P2} K_{pm} / R_{P1})}{J_m J_L}, \\ a_0 &= \frac{(G_R R_{P1} R_{P2} K_b K_{il} + G_R R_{P2} K_{im} / R_{P1})}{J_m J_L}. \end{aligned} \quad \{20\}$$

$$\begin{aligned}
\Psi_{mLr}(s) &= s^4 + f_3s^3 + f_2s^2 + f_1s + f_0, \\
f_3 &= \frac{(b_m J_L + J_m b_L + J_L K_{pm})}{J_m J_L}, \\
f_2 &= \frac{(K_b J_{eq} + b_m b_L + K_{pm} b_L + J_L K_{im})}{J_m J_L}, \\
f_1 &= \frac{(K_b b_{eq} + G_R^2 K_b K_{pm} + K_{im} b_L + G_R R_{P1} R_{P2} K_b K_{pL})}{J_m J_L}, \\
f_0 &= \frac{K_{im} G_R^2 R_{P2}^2 K_b + G_R R_{P1} R_{P2} K_b K_{iL}}{J_m J_L}.
\end{aligned} \tag{21}$$

Note that the coefficients  $f_0$  to  $f_3$  depend on the gains of the control law. Singular perturbation analysis for this case results in the slow and fast characteristic polynomials as

$$\Psi_{mLs}(s, \varepsilon) \approx s^2 + \gamma_1 s + \gamma_0 \tag{22a}$$

$$\Psi_{mLf}(p, \varepsilon) \approx p^2 + \gamma'_1 p + \gamma'_0 \tag{22b}$$

where

$$\begin{aligned}
\gamma_1 &= \frac{G_R^2 R_{P2}^2 b_m + R_{P1}^2 b_L + G_R R_{P2} R_{P1} K_{pL} + G_R^2 R_{P2}^2 K_{pm}}{G_R^2 R_{P2}^2 J_m + R_{P1}^2 J_L}, \\
\gamma_0 &= \frac{G_R^2 R_{P2}^2 K_{im} + G_R R_{P2} R_{P1} K_{iL}}{G_R^2 R_{P2}^2 J_m + R_{P1}^2 J_L}, \\
\gamma'_1 &= \frac{G_R^2 R_{P2}^2 b_m + R_{P1}^2 b_L + G_R^2 R_{P2}^2 K_{pL} + G_R^2 R_{P2}^2 K_{pm} (J_L/J_m)}{G_R^2 R_{P2}^2 J_m + R_{P1}^2 J_L} \varepsilon, \\
\gamma'_0 &= \frac{G_R^2 R_{P2}^2 J_L + R_{P1}^2 J_m}{J_m J_L}.
\end{aligned} \tag{23}$$

Therefore, the slow and fast subsystems are stable for all positive controller gains. Note that the outputs of both load speed and motor speed controller combine to form a torque input to the motor; this is typically referred to as the torque mode in practice when multiple loops such as this are employed. Another strategy is to use the output of the load speed controller as the motor speed reference correction. But this strategy results in an unstable system which is shown in [6].

## WEB TENSION CONTROL

Consider a rewind section as shown in Figure 6. The web span tension dynamics in the rewind section is given by

$$\dot{t}_3 = \frac{EA_w}{L_3} (v_3 - v_2) + \frac{1}{L_3} (t_2 v_2 - t_3 v_3). \tag{24}$$

The periodic torque disturbance is injected on the load side of the rewind roll by employing a brake on the roll shaft. The disturbance is expressed in the

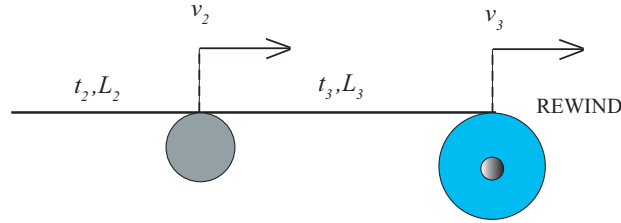


Figure 6 – Rewind section

form of equation {25}. The injected disturbance affects the velocity  $v_3$  and as a consequence the web tension  $t_3$ . The relation between the web velocity  $v_3$  and web tension  $t_3$  can be seen through equation {24}. It is assumed that the velocity  $v_2$  is well regulated. The proposed load speed regulation scheme is applied to rewind roll to regulate velocity  $v_3$  in the presence of disturbance on load side and this control scheme is expected to regulate web tension due to dynamics between velocity and tension.

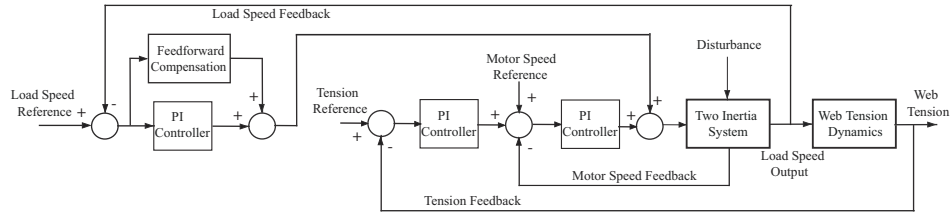


Figure 7 – Load speed control scheme for web tension control

The use of feedforward compensation to reject known disturbances by direct cancelation or unknown disturbances by their estimation has been known to be effective in attenuating disturbances. We consider the rejection of periodic disturbances on the load by using an adaptive feedforward action based on load speed error. The control scheme that utilizes the feedforward action is shown in Figure 7.

We use an adaptive feedforward algorithm given in [4] that is particularly applicable in this situation as the feedforward action preserves the stability of the overall system with the feedback controller with simultaneous motor and load speed feedback. The approach is briefly discussed as applicable to this problem; the details are given in [4]. The idea is to estimate the amplitude and phase of the disturbance for a known frequency of the disturbance. The disturbance can be expressed in the form

$$\begin{aligned}
 d &= \theta_1^* \cos(\omega t) + \theta_2^* \sin(\omega t) \\
 &:= \phi(t)w_0^*
 \end{aligned}
 \tag{25}$$

where  $\omega$  is a known frequency,  $\theta_1^*$  and  $\theta_2^*$  are unknown parameters, and

$\phi(t) = [\cos(\omega t) \quad \sin(\omega t)]$ ,  $w_0^* = [\theta_1^* \quad \theta_2^*]$ . The adaptation laws for the unknown parameters  $\theta_1^*$  and  $\theta_2^*$  are given by the following simple pseudo-gradient algorithm:

$$\dot{\theta}_1 = \gamma e(t) \cos(\omega t), \quad \{26a\}$$

$$\dot{\theta}_2 = \gamma e(t) \sin(\omega t), \quad \{26b\}$$

where  $\theta_1$  and  $\theta_2$  are the parameter estimates,  $e(t) = \omega_{rL} - \omega_L$  is the load speed error, and  $\gamma$  is the adaptation gain. Since the regressor vector  $\phi(t)$  is persistently exciting, the parameter vectors converge to zero. In fact, this adaptive feedforward action with estimation of disturbance parameters using the pseudo-gradient algorithm has been shown to be equivalent to the use of the internal model of the disturbance in [4]. Using the estimated parameters, the feedforward control action is given by

$$u_f = -\theta_1 \cos(\omega t) - \theta_2 \sin(\omega t). \quad \{27\}$$

## EXPERIMENTS

Pictures of the experimental setup are shown in Figure 8. It consists of an AC motor shaft connected to the load shaft (roll) via a belt-pulley and gear-pair transmission. A 15 HP (11.19 KW) AC motor with a rated speed of 1750 RPM is employed. The transmission ratio ( $BR = (R_2/R_1)G_R$ ) is 3.825. An encoder on the motor shaft is employed to measure the motor shaft speed and a laser sensor is used to measure the load shaft speed. The real-time hardware, including the drives, controller, and communication network, was provided by Rockwell Automation (Allen-Bradley). All the real-time hardware components of the machine are connected through a ControlNet communication network. The network is updated every 5 ms (Network Update Time) and data is communicated to the network every 10 ms (Request Package Interval). A brake is attached on the other side of the load shaft to inject periodic torque disturbances; a magnetic clutch brake (Magpower GBC 90) that can apply 26 lb-ft torque is used.

The PI controller gains for the motor speed loop were chosen to be  $K_{pm} = 15$  and  $K_{im} = 3.09$  and for the load speed loop to be  $K_{pL} = 0.07$  and  $K_{iL} = 0.001$ . Experiments were conducted at different reference speeds to evaluate the performance of proposed control scheme. In each experiment, the brake provides an external periodic disturbance torque of the form  $A + B \sin(\omega_d t)$  ( $A = 2, B = 1.5$ ). The following disturbance frequencies were injected to evaluate the control schemes:  $\omega_d = 0.05, 0.15, 0.25$  Hz. These disturbances are typical of the disturbances that are observed in roll-to-roll manufacturing machines where such transmission systems are typically employed. The adaptation gain  $\gamma = 1$  is chosen and the initial value of the estimates is assumed to be zero.

The proposed control scheme is extended to an R2R system and implemented in the rewind section of experimental platform shown in Figure 9. The experiments are performed at web speed reference of 150 FPM and 200

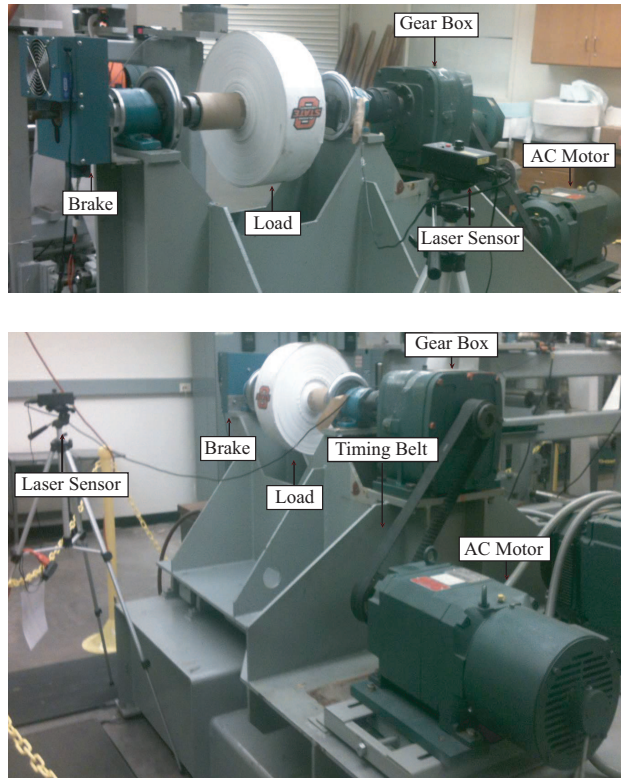


Figure 8 – Pictures of the experimental platform. Top: Load side. Bottom: Motor side.

FPM, and web tension reference of 20 lbf. A disturbance torque of the form  $A + B \sin(\omega_d t)$  ( $A = 1.3, B = 1$ ) is applied using a brake attached on the load side. Disturbances of frequencies 0.25 Hz and 0.3 Hz are injected at 150 FPM and 200 FPM, respectively. The upstream pull roll to the rewind section is under pure speed control. The proposed motor and load speed feedback control scheme with adaptive feedforward is applied to the rewind roll and compared with a commonly used motor speed feedback scheme. The tension and velocity response real-time data are collected for each scenario.

Figure 10 shows the evolution of the load speed (reflected to the motor side) in the presence of disturbance with frequency 0.25 Hz when the reference speed is 719 RPM with and without the use of the adaptive feedforward action. Figure 11 shows the Fast Fourier Transform (FFT) of the load speed for the two cases. It is evident that the control scheme with the AFF action can provide significantly improved load speed regulation. Figure 12 provides control torque input corresponding to the two cases, without and with adaptive feedforward compensation. It is evident that the torque input is larger when the adaptive feedforward is employed. Table 1 shows the standard deviation of the load speed

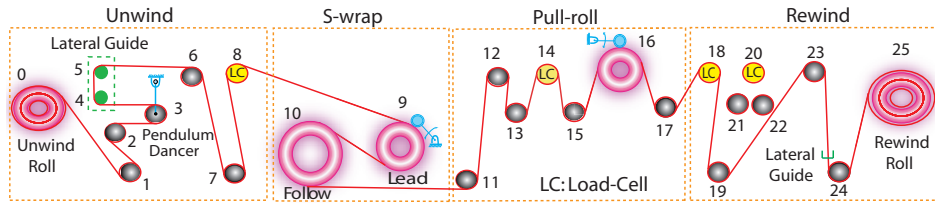


Figure 9 – Schematic of R2R experimental setup

signal from its reference for the various schemes. It is clear that the employing load speed feedback in addition to motor speed feedback can improve performance. Further, use of the adaptive feedforward action based on load speed feedback can significantly improve the regulation performance.

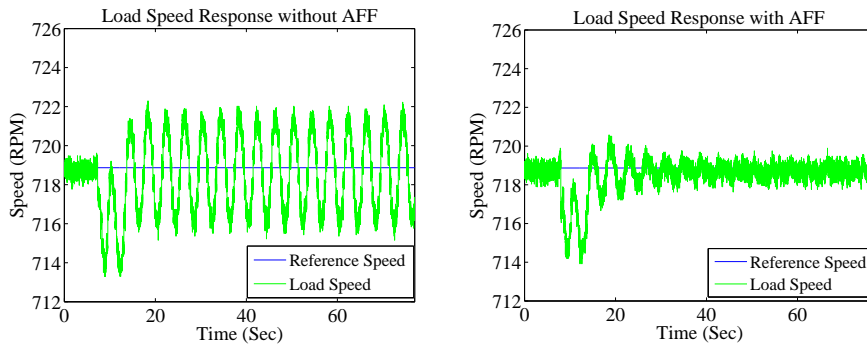


Figure 10 – Load speed response with 0.25 Hz torque disturbance. Top: Without AFF. Bottom: With AFF

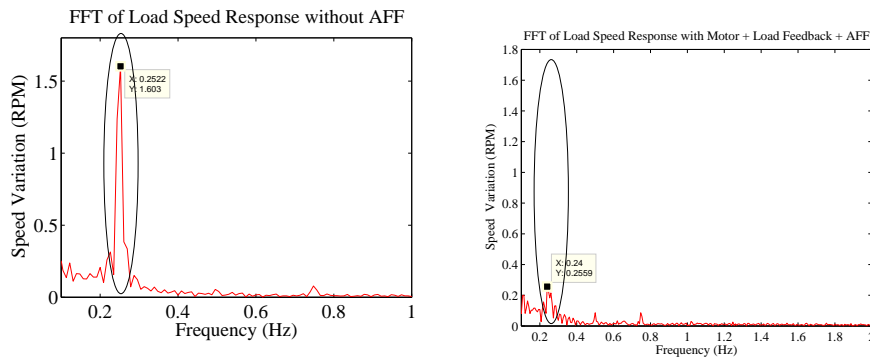


Figure 11 – FFT of load speed response with and without AFF

Figure 13 shows web tension response in the presence of disturbance with

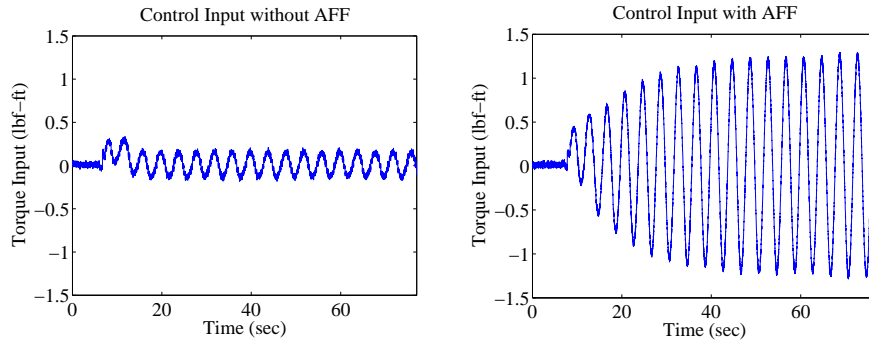


Figure 12 – Control input with 0.25 Hz torque disturbance. Top: Without AFF. Bottom: With AFF

Table 1 – Comparison of different control schemes

Disturbance Frequency	Standard Deviation		
	Only Motor Feedback	Motor + Load Feedback	Motor + Load Feedback + AFF
0.25 Hz	2.09	1.35	0.34
0.15 Hz	4.71	3.53	0.87
0.05 Hz	3.89	2.47	0.68

frequency 0.25 Hz at 150 FPM. The control strategy that uses only motor speed was unable to attenuate the disturbance which is reflected in the tension response (shown in top plots of Figure 13). The motor and load speed feedback control scheme attenuates disturbance in tension response; however the attenuation is not significant (shown in middle plots of Figure 13). The proposed control scheme with feedforward action rejects the disturbance and regulates the tension to its desired value (shown in bottom plots of Figure 13).

Figure 13 also shows the FFT of the tension response with three separate control schemes. The proposed control scheme attenuates the disturbance amplitude at 0.25 Hz significantly. Figure 14 shows corresponding load and motor speed response in the presence of disturbance at 150 FPM. Similar results can be seen at 200 FPM which are provided in Figures 15 and 16.

## CONCLUDING REMARKS

We have investigated the problem of regulating load speed in a mechanical transmission with a compliant belt. This problem is important in many industries where such transmission systems are employed, and practicing engineers often grapple with the question of whether to use motor speed feedback or load speed feedback to regulate the load speed. Singular perturbation analysis of the system shows that pure load speed feedback is not

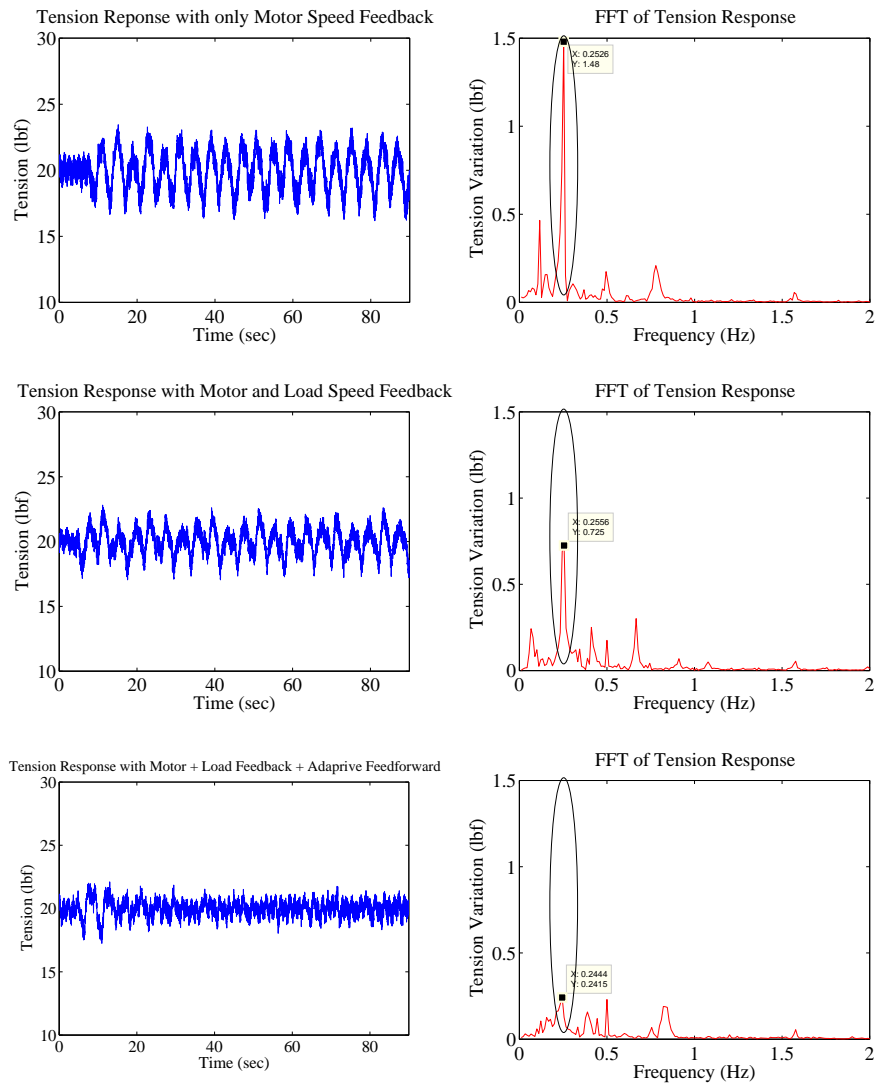


Figure 13 – Tension response and FFT of tension response with 0.25 Hz torque disturbance; Top: only motor feedback, Middle: motor + load feedback, Bottom: motor + load feedback + AFF

stable and must be avoided. To directly control the load speed, we have also considered a scheme that utilizes both motor and load speed feedback that is stable. Since the feedback control action is not sufficient to reject periodic load disturbances, we have also considered a suitable adaptive feedforward algorithm that utilizes estimation of the disturbance and provides compensation term to reject the disturbance. Experiments were conducted on an industrial grade



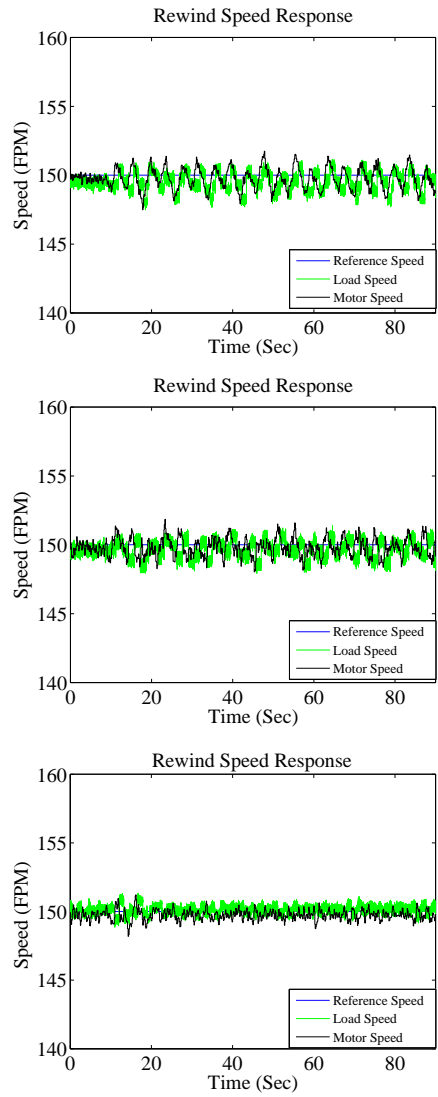


Figure 14 – Load speed and motor speed response at 150 FPM with 0.25 Hz disturbance; Top: only motor feedback, Middle: motor + load feedback, Bottom: motor + load feedback + AFF

transmission system to evaluate the control schemes and compare their performance. Although we have used only belt compliance as the compliant element in the transmission system, torsional compliance due to long shafts can also be included and the analysis conclusions will remain the same. The proposed load speed control scheme gives desired web tension performance by rejecting disturbance in the rewind section.

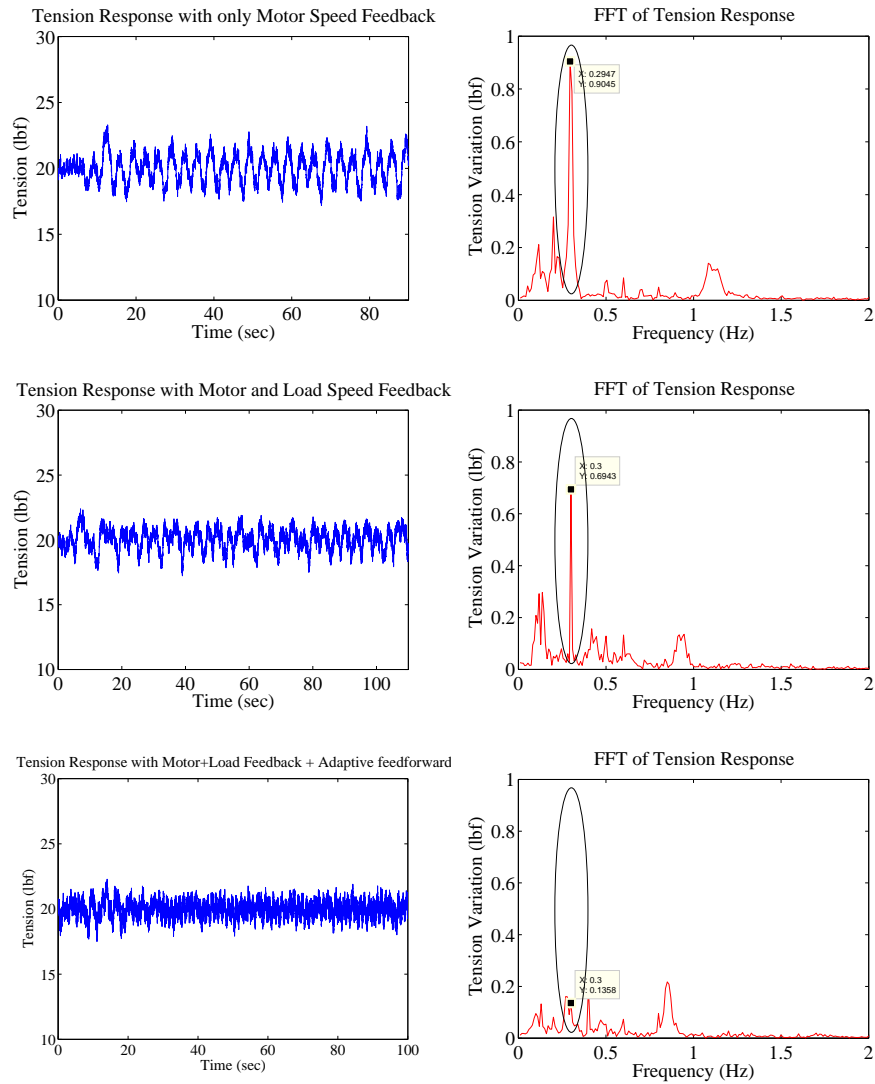


Figure 15 – Tension response and FFT of tension response with 0.3 Hz torque disturbance; Top: only motor feedback, Middle: motor + load feedback, Bottom: motor + load feedback + AFF

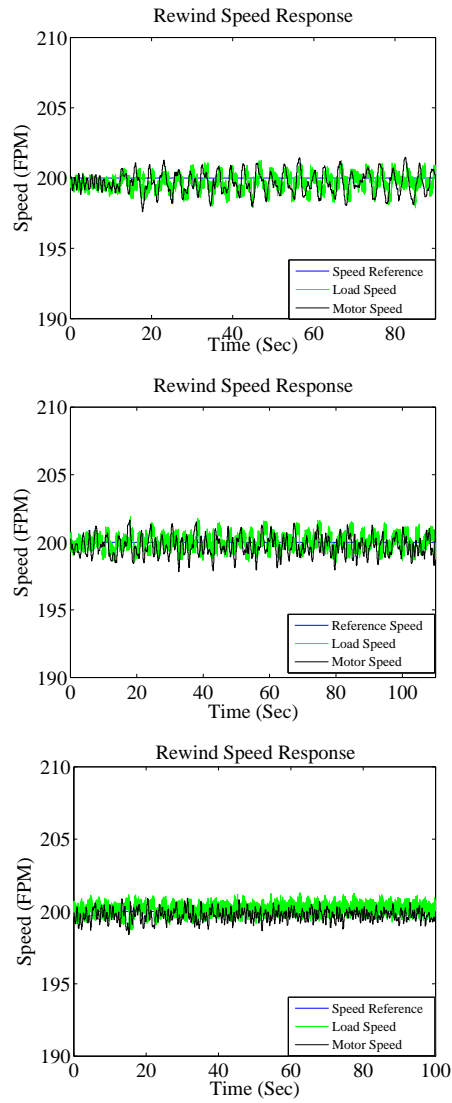


Figure 16 – Load speed and motor speed response at 200 FPM with 0.3 Hz disturbance; Top: only motor feedback, Middle: motor + load feedback, Bottom: motor + load feedback + AFF

## ACKNOWLEDGEMENTS

This work was supported by the Web Handling Research Center, Oklahoma State University, Stillwater, Oklahoma.

## REFERENCES

1. Dwivedula, R. V., and Pagilla, P. R., "Effect of Backlash on Web Tension in Roll-to-Roll Manufacturing Systems: Mathematical Model, Mitigation Method and Experimental Evaluation," IEEE Multi-conference on Systems and Control, February 2013.
2. Kokotovic, P., Khalil, H. K., and O'Reilly, J. O., "Singular Perturbation Methods in Control: Analysis and Design," Society for Industrial and Applied Mathematics edition, Academic Press, London, First ed., 1986.
3. Dubowsky, S., and Freudenstein, F., "Dynamic Analysis of Mechanical Systems with Clearance: Part 1: Formulation of Dynamic Model," ASME Journal of Engineering for Industry, vol. 93, February 1971, pp. 305-309.
4. Bodson, M., "Rejection of Periodic Disturbances of Unknown and Time-varying Frequency," International Journal of Adaptive Control and Signal Processing, vol. 19, 2005, pp. 67-88.
5. Bradenburg, G., and Schafer, U., "Design and Performance of Different Types of Observers for Industrial Speed and Position Controlled Electromechanical Systems," Proc. Int. Conf. of Electrical Drives and Power Electronics, Slovakia, 1990, pp. 1-10.
6. Dwivedula, R. V., "Modeling the Effects of Belt Compliance, Backlash, and Slip on Web Tension and New Methods for Decentralized Control of Web Processing Lines," Phd thesis, Oklahoma State University, Stillwater, OK, December 2005.
7. Freeman, E. A., "The stabilization of control systems with backlash using a high-frequency on-off loop," The institute of Electrical Engineers, vol. 356, February, 1960, pp. 150-157.
8. EI-Sharkawi, M., and Guo, Y., "Adaptive Fuzzy Control of a Belt-driven Precision Positioning Table," In Proceedings of the IEEE International Electric Machines and Drives Conference, vol. 3, June, 2003, pp. 1504-1506.
9. Pagilla, P. R., Siraskar, N. B., and Dwivedula, R. V., "Decentralized Control of Web Processing Lines," IEEE Transactions on Control Systems Technology, vol. 15, January 2007, pp. 106-117.
10. Pagilla, P. R., Dwivedula, R. V., and Siraskar, N. B., "A Decentralized Model Reference Adaptive Controller for Large-scale Systems," IEEE Transactions on Mechatronics, vol. 12, April 2007, pp. 154-163.